

pubs.acs.org/est Article

# Wildfire Ashes from the Wildland-Urban Interface Alter Vibrio vulnificus Growth and Gene Expression

Karlen Enid Correa Velez, Mahbub Alam, Mohammed A. Baalousha, and R. Sean Norman\*



Cite This: Environ. Sci. Technol. 2024, 58, 8169–8181



**ACCESS** I

III Metrics & More

Article Recommendations

s Supporting Information

ABSTRACT: Climate change-induced stressors are contributing to the emergence of infectious diseases, including those caused by marine bacterial pathogens such as *Vibrio* spp. These stressors alter *Vibrio* temporal and geographical distribution, resulting in increased spread, exposure, and infection rates, thus facilitating greater *Vibrio*—human interactions. Concurrently, wildfires are increasing in size, severity, frequency, and spread in the built environment due to climate change, resulting in the emission of contaminants of emerging concern. This study aimed to understand the potential effects of urban interface wildfire ashes on *Vibrio vulnificus* (*V. vulnificus*) growth and gene expression using transcriptomic approaches. *V. vulnificus* was exposed to structural and vegetation ashes and analyzed to identify differentially



expressed genes using the HTSeq-DESeq2 strategy. Exposure to wildfire ash altered *V. vulnificus* growth and gene expression, depending on the trace metal composition of the ash. The high Fe content of the vegetation ash enhanced bacterial growth, while the high Cu, As, and Cr content of the structural ash suppressed growth. Additionally, the overall pattern of upregulated genes and pathways suggests increased virulence potential due to the selection of metal- and antibiotic-resistant strains. Therefore, mixed fire ashes transported and deposited into coastal zones may lead to the selection of environmental reservoirs of *Vibrio* strains with enhanced antibiotic resistance profiles, increasing public health risk.

KEYWORDS: Vibrio vulnificus, wildland-urban interface, fire ashes, transcriptomic, climate change, antibiotic resistance, metal resistance

#### 1. INTRODUCTION

Climate change is causing unprecedented ecological changes and affecting the environment at different levels worldwide. For example, ocean surface warming has accelerated in the past decade to 0.280 ± 0.068 °C per decade, the ocean pH has declined (0.1 since the Industrial Revolution), and the sea level has increased by 3.3  $\pm$  0.4 mm yr<sup>-1.1,2</sup> These effects are especially pronounced in coastal areas experiencing climatelinked stressors such as temperature increases, sea-level rise, altered salinity and pH, and increased frequency of anomalous weather events.<sup>3,4</sup> These climate-linked stressors are altering temporal and geographical distribution patterns in diseases sensitive to environmental changes, such as Vibrio infections, including those caused by Vibrio vulnificus (V. vulnificus) and Vibrio parahemolyticus. 5-7 During the past decades, the number of Vibrio infections has increased in the United States, and the same trend has been observed worldwide, even in higher latitudes where environmental conditions previously were considered adverse for Vibrio proliferation.8-12 Vibrio usually inhabits warm (≥15 °C) estuarine and marine environments with low and moderate salinity (5 to 25 ppt), where temperature and salinity modulate the distribution and abundance. 13-17 The poleward spread and the increase in Vibrio infections have been correlated with the altered geographical constraints driven by warming seawater temperatures and sea-level rise, increasing the human disease burden globally. 6,18 The model developed by Archer et al. indicated that climate change has affected V. vulnificus infection distribution and the number of cases in the Eastern USA.<sup>18</sup> Another study examined vibriosis cases following the landfall of Hurricane Ian in Florida, which resulted in 38 cases and 11 vibriosis-associated deaths. 19 In addition to anomalous rainfall and storm surge, changes in sea surface temperature and chlorophyll concentration during and after the hurricane favored Vibrio growth, increasing Vibrio-human interactions.<sup>20</sup> From a public health perspective, Vibrio vulnificus is the greatest concern because it is responsible for more than 95% of seafood-related deaths in the USA.<sup>21</sup> V. vulnificus is an invasive opportunistic pathogen for humans and marine animals that

Received: October 18, 2023 Revised: April 18, 2024 Accepted: April 22, 2024 Published: May 1, 2024





can be transmitted by contact or ingestion. While not all strains are pathogenic, those that can cause infection typically possess specific virulence factors, including acid neutralization, capsular polysaccharide expression, iron acquisition, cytotoxicity, motility, and the expression of certain proteins involved in attachment and adhesion.<sup>21</sup> The presence of these factors has been linked to increased pathogenicity.<sup>22</sup> V. vulnificus uses acid neutralization mechanisms, such as the cadBA system, to survive in acidic environments such as the human stomach when ingested.<sup>23</sup> V. vulnificus capsular polysaccharide expression plays a critical role in the evasion of the host immune system by conferring an antiphagocytic ability and resistance to complement-mediated killing.<sup>24</sup> V. vulnificus obtains iron from blood through various iron acquisition systems that can enhance growth and proliferation in the host.<sup>25</sup> Studies analyzing the transcriptome of diverse biotypes of V. vulnificus have revealed that external factors such as environmental cues, nutrient levels, and temperature can activate a host-specific virulence profile.  $^{26-30}$  Exposure to these abiotic and biotic stressors activates Vibrio response and adaptative mechanisms to colonize and persist in natural environments and provides preadaptation for survival in a human host. 27,31,32 Studies have correlated the occurrence of pathogenic Vibrio with changes in environmental parameters and anthropogenic pressures.<sup>33</sup> Recent studies suggest that V. vulnificus populations can be classified into four distinct clusters as a result of their genetic diversity, ecological characteristics, and ecological selective pressures that contribute to the emergence of new strains. This finding has led to concerns regarding the potential emergence of strains with increased virulence potential due to their high genome plasticity.<sup>34,35</sup> It has been suggested that climate hazards, demographic changes, and population growth in coastal areas are key factors in the increase in Vibrio-human interactions. 36,18

Climate change is also impacting wildfires, which are increasing in size, severity, frequency, and spread into the built environment, resulting in the emission of contaminants of emerging concern. 37-39 When a fire occurs, various pollutants are released and become concentrated in the ashes, which include metals, metalloids, incidental nanomaterials, chemicals, and organic contaminants, among other substances. 40,41 Wildfires that occur at the wildland-urban interface (WUI), where the built environment and wildland vegetation intermingle, release construction-related chemicals into the environment, posing a significant threat to water and air quality, as well as the health of individuals in the surrounding areas. 42,43 For example, the ashes produced by a burned building in the WUI can contain high levels of different trace metals such as Pb, Cr, As, Cu, and Zn. 44,45 Ashes with elevated concentrations of Cr, As, and Cu can be generated from chromated copper arsenic-treated wood that has been used for construction since 1930. 46,47 Fire ashes enriched with these metals and other contaminants can be broadly transported through smoke plumes and runoff into ecosystems suitable for Vibrio proliferation, creating a potential mechanism that may alter Vibrio growth patterns and virulence profiles. To date, there is limited information about how these fire-emitted contaminants can affect the bacterial communities in estuaries and coastal zones, including Vibrio spp.

This study examined the potential effect of wildfire ashes on *Vibrio* growth by exposing a strain of *V. vulnificus* to different wildfire ashes from the wildland-urban interface zone and using transcriptomic analysis to identify genes and mechanisms that

are differentially regulated in the presence of structural and vegetation ashes. A better understanding of how *V. vulnificus* responds to the input of wildfire ashes and the mechanisms involved will aid in the development of comprehensive models for predicting potential *Vibrio* outbreaks, raising health risk awareness in coastal regions.

# 2. MATERIALS AND METHODS

**2.1. Fire Ash Description.** Two fire ashes representing structural (A24) and vegetation ashes (A31) were used to examine the potential impact of wildland-urban interface fire ashes on coastal microbial communities using the type strain V. vulnificus 324 (ATCC 27562) as a model of an opportunist human and animal pathogen. V. vulnificus serves as a model organism for studying coastal microbial communities because it naturally occurs in estuarine and coastal environments, and its presence and abundance are closely tied to environmental factors, especially temperature, salinity, and nutrient availability. Monitoring V. vulnificus populations helps assess the impact of climate change and pollution on coastal microbial communities. V. vulnificus can also cause severe infections in humans, making it a useful model to understand the interactions between human health and coastal conditions. This strain was isolated from the blood of an individual following exposure to seawater containing lactose-positive, halophilic Vibrio bacteria and has been used as a reference for clinical strains.<sup>48</sup> The fire ashes were collected from the LNU Lightning Complex Fire site that burned during the 2020 California fire season. Samples were collected prior to any rain or other precipitation with disposable plastic scoops and placed in zippered plastic bags. The structural ash used in this study was a dark-green ash sample that was collected from a burned residential structure foundation and is representative of structural ash originating from copper-chromated arsenatetreated wood. While the chemical composition of structural ash varies significantly by the burned material, the structural ash used in this study is representative of the copper chromate arsenate-treated wood ashes that have been reported in other wildland-urban interface fires. A31 vegetation ash is gray ash from burned chaparral (charred manzanita and some pine) that represents the typical chemical composition found in vegetation ash in wildfires. The elemental compositions of A24 structural ash and A31 vegetation ash are presented in detail in previous publications. 45,49 The A24 and A31 ashes described in the previous publications are referred to as structural and vegetation ash, respectively, in the subsequent sections of this manuscript. Briefly, the elemental composition of structural ash is characterized by high concentrations of Cr (183  $\pm$  15 g of  $kg^{1-}$ ), Cu (116 ± 17 g of  $kg^{1-}$ ), and As (44 ± 4 mg of  $kg^{1-}$ ). Cr, Cu, and As account for 91% of the concentrations of all measured elements. In contrast, the elemental composition of vegetation ash is characterized by high concentrations of Fe  $(62 \pm 3 \text{ g kg}^{1-})$ , Al  $(28 \pm 2 \text{ g kg}^{1-})$ , and Ca  $(16 \pm 2 \text{ g kg}^{1-})$ , which account for 93.3% of the concentrations of all measured elements (Figure S1).

**2.2.** Concentration—Response Analysis of the Effect of Fire Ashes on *V. vulnificus*. To define the sublethal concentration of fire ash to be used in subsequent *V. vulnificus* transcriptomic studies, a dose—response experiment was performed to assess the effect of the fire ash concentration on bacterial growth. *V. vulnificus* was grown at 30 °C in 96-well plates containing three replicates of each fire ash condition. Experimental conditions consisted of different amounts of fire

ash suspended in modified seawater yeast extract (MSYE), giving final culture media concentrations of 0 (control), 5, 10, 25, 50, 75, 100, and 150 mg  $L^{-1}$  based on the Cu and Fe content in structural ash and vegetation ash, respectively. 50 For the structural ash, concentrations were based on the Cu content due to its common use as a biocide and background studies examining the minimal inhibitory concentrations across a range of bacteria, providing an initial range for the V. vulnificus concentration-response analysis. The fire ash amount and the relevant metal content concentrations for all conditions are shown in Table S1. Modified seawater yeast extract was used to provide a sufficient carbon source to assess the effect of fire ash on bacterial growth. In the experimental conditions, 10 µL of diluted 1:10 overnight fresh V. vulnificus culture (8 h) was used as an inoculum, and no bacteria-added controls were included as negative controls. The optical density at 600 nm (OD<sub>600</sub>) of each replicate was measured hourly for 24 h using a Victor X3 plate reader (PerkinElmer, Waltham, MA, USA) to determine bacterial growth. The background-subtracted OD data was used to model growth curves using the Gaussian process regression, and modelpredicted OD's were used to estimate the growth rate for each treatment using the Analysis of Microbial Growth Assays (AMiGA) program. 51 The bacterial growth rates of V. vulnificus obtained from the AMiGA analysis were calculated as  $\left(\frac{d}{dt}\ln OD\right)$ . Different models were tested to find the best fit using the "drc" package in R.52 The growth rate data were fitted using a four-parameter log-logistic model (LL.4) with the lower limit equal to 0 to restrict the model parameters to biologically relevant estimates and determine the half-maximal effective concentration (EC<sub>50</sub>) values.<sup>52</sup> The EC<sub>50</sub> values were compared using the "EDcomp" function, where the null hypothesis was that the ratio equals 1. The dose-response model was visualized with the "plot" function using R and RStudio. 52-54

2.3. Fire Ash Exposure Transcriptomic Study. To examine the effects of wildland-urban interface fire ashes on bacterial growth and gene expression, V. vulnificus was initially grown in MSYE at 30 °C until it reached the exponential phase (OD 0.4). One mL of the V. vulnificus culture was then used as an inoculum in 59 mL of ash suspension media for the structural and vegetation ash conditions, obtaining a final dilution of 1:60 (v/v) of the culture (Figure S2). Sublethal exposure conditions consisted of MSYE with a suspension of A24 structural ash (12.75 mg of ash in 60 mL of media equivalent to ~25 mg  $L^{-1}$  Cu, ~39 mg  $L^{-1}$  Cr, and ~9 mg  $L^{-1}$ As) and A31 vegetation ash (22.87 mg of ash in 60 mL of media equivalent to  $\sim$ 25 mg L<sup>-1</sup> Fe,  $\sim$ 11 mg L<sup>-1</sup> Al, and  $\sim$ 6 mg L<sup>-1</sup> Ca). Briefly, a given mass of ash was suspended in 60 mL of MSYE media to obtain the final metal concentrations stated above. Dissolved metal concentrations were allowed to reach equilibrium prior to Vibrio inoculation to ensure exposure to similar metal states (dissolved versus particulate) across all experimental conditions. Exposure cultures were grown in 250 mL flasks for 24 h at 30 °C with shaking at 220 rpm, and three biological replicates were performed for each condition. No bacteria-added cultures were also included as a control. The OD<sub>600</sub> of the cultures was measured every 2 h for structural ash and hourly for vegetation ash using a Victor X3 plate reader to determine the bacterial growth stage. At three different time points (8, 16, and 24 h for structural ash and 3, 6, and 8 h for vegetation ash), 10 mL of each culture was

collected and treated with Qiagen RNAprotect (Qiagen, Germantown, MD, USA) for immediate RNase inactivation and RNA stabilization to preserve the gene expression profile. RNA-stabilized samples were centrifuged at 6000g for 10 min, and the cell pellets were used for nucleic acid extraction. To ensure that the samples were collected from similar growth stages, the collection time point differs between the two fire ashes based on the bacterial growth rate. In addition, 4 mL of each culture was collected and filtered for the dissolved metal analysis.

2.4. RNA Extraction, Library Preparation, and Sequencing. RNA was extracted using an RNeasy Mini kit (Qiagen, Germantown, MD, USA) following the manufacturer's instructions. Briefly, three replicates of each condition were performed, and total RNA was extracted from cell pellets of structural and vegetation ash cultures. Gene expression analysis was limited to the 3 (vegetation ash) and 8 h (structural ash) time points (OD<sub>600</sub>: 0.024 for vegetation ash and 0.069 for structural ash) to obtain samples from similar growth stages and minimize the effect of growth stagedependent gene expression. The RNA samples extracted from the additional time points not included in the analysis (16 and 24 h for the structural ash condition and 6 and 8 h for vegetation ash) were stored at -80 °C. RNA quantity was measured using a NanoDrop spectrophotometer (Thermo Fisher Scientific, Waltham, MA, USA) and a Qubit RNA highsensitivity assay (Invitrogen by Thermo Fisher Scientific, Waltham, MA, USA). Ribosomal RNA was depleted from the total RNA using an NEBNext rRNA depletion kit (New England Biolabs, Ipswich, MA, USA), and the quality and quantity of the remaining mRNA were assessed using an Agilent bioanalyzer (Agilent Technologies, Santa Clara, CA, USA) with the RNA 6000 Pico assay. Purified mRNA was used to prepare individually barcoded RNA-seq libraries using an NEBNext Ultra II directional RNA library prep kit (New England BioLabs, Ipswich, MA, USA) according to the manufacturer's instructions for intact RNA (RNA integrity number (RIN) > 7). All the samples used in this study had a RIN  $\geq$  7.2. The RNA-seq libraries were sequenced on an Illumina HiSeq DNA sequencer with 2 × 150 bp paired-end reads. All raw sequencing data were deposited into the Genbank Sequence Read Archive (SRA) database under the BioProject accession number PRJNA1010168.

2.5. RNA-seq Analysis and Visualization. Raw sequence reads were quality and adapter trimmed using fastp (v.0.20.0) with the following parameters: --3 (drop the bases in the 3' end if the mean quality is lower of the cut mean quality) and -y (low complexity filter) (Table S2).55 Cleaned RNA-seq reads were aligned against the V. vulnificus NBRC 15645 reference genome (GenBank Accessions: CP012882.1 and CP012881.1), annotated, and analyzed to find differentially expressed genes using the HTSeq-DESeq2 strategy in the Bacterial and Viral Bioinformatic Resource Center (BV-BRC) analysis tool.<sup>56</sup> The HTSeq-DESeq2 strategy used Bowtie 2, HTSeq, and DESeq2 to align, estimate abundance and raw counts, and compare samples, respectively. 57-59 The default parameters were used for transcript analysis. DESEq2 calculated the Log2 fold change and the fold change significance. The no-ash condition (control) was treated as the baseline condition for the analysis. The statistical significance threshold for differential gene expression was an FDR-adjusted *p*-value less than or equal to 0.05.

To visualize the significantly different expressed genes during the exposure, a heat map was generated from the transcript per million (TPM) values using the Complex-Heatmap package using the "Heatmap" function, and functional categories were visualized using the "ggplot2" package using R and RStudio. <sup>53,54,60–62</sup> A principal component analysis (PCA) was generated to visualize the differences among the treatments in an overall analysis using the "prcomp" function and the "ggbiplot" package in R and RStudio. <sup>53,54,63</sup> The PCA values were calculated from the gene expression (TPM values) across the sample conditions.

2.6. Dissolved Metal Concentration. Four mL of each culture containing the A24 and A31 suspension was filtered through a 3 kDa Amicon ultracentrifugal filter (Merck Millipore Ltd., Ireland) by centrifugation at 4000 rpm for 20 min. The filtrates were acidified by adding 0.57  $\mu$ L of distilled HNO<sub>3</sub> (trace metal grade, Fisher Chemical, Fair Lawn, NJ, USA) to obtain a final concentration of 1% HNO<sub>3</sub>. The metal concentrations were determined using an inductively coupled plasma-time-of-flight-mass spectrometer (ICP-TOF-MS, TOF-WERK, Thun, Switzerland). Mass spectral calibration and routine tuning were performed before analysis to achieve maximum sensitivity. Elemental concentration calibration was established using a series of ionic standards prepared in 1% HNO3 from commercially available ICP multielement standards (BDH Chemicals, Radnor, PA, USA) with concentrations ranging from 0.001 to 100  $\mu$ g L<sup>-1</sup>. Internal standards (ICP Internal Element Group Calibration Standard, BDH Chemicals, Radnor, PA, USA) were used to monitor the signal drift for quality control. The instrument operating conditions are presented in Table S3, and the monitored isotopes are listed in Table S4.

## 3. RESULTS AND DISCUSSION

**3.1.** Vibrio vulnificus Growth Rate Follows a Dose-Dependent Response to Fire Ash Concentration. The dose—response curves of the effects of fire ashes on *V. vulnificus* showed a decreasing growth rate as a function of increasing fire ash concentrations, suggesting that both fire ashes are toxic and

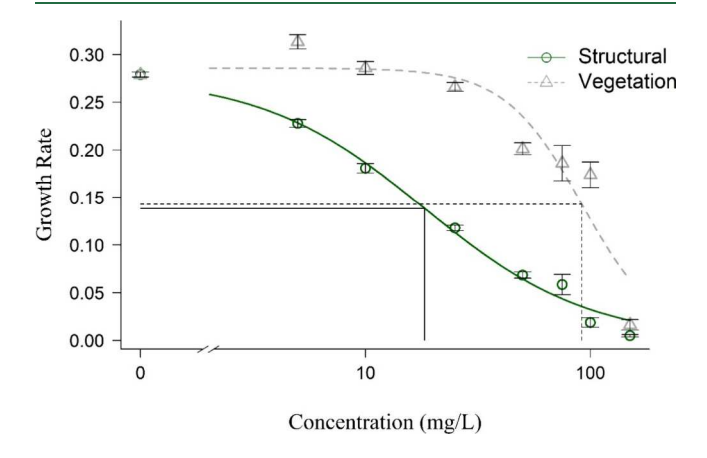


**Figure 1.** Concentration—response curve of the V. vulnificus growth rate after exposure to different structural and vegetation fire ash concentrations. The regression curves were modeled using a four-parameter log—logistic model function. The predicted model and the  $EC_{50}$  value for structural ash are shown as a solid line and for vegetation ash as a dashed line. The mean of the observed growth rate is represented by a circle (structural ash) and a triangle (vegetation ash).

suppress bacterial growth at different levels (Figure 1). The EC<sub>50</sub> value of structural ash (18.32  $\pm$  4.38 mg L<sup>-1</sup>) was five times lower than that of vegetation ash (91.56  $\pm$  11.77 mg L<sup>-1</sup>), indicating that the structural ash resulted in higher toxicity to *V. vulnificus*. The estimated ratio of the EC<sub>50</sub> values (0.20009) differs from 1, rejecting the null hypothesis, meaning that the EC<sub>50</sub> values are significantly different (p < 0.001). The level of toxicity of the fire ash is suggested to be determined by the fire ash composition.

The dose-response analysis showed that the fire ashes, structural and vegetation, differ in toxicity, suggesting differences in bacterial growth parameters. The dose-response also suggested that the 25 mg L<sup>-1</sup> concentration based on the Cu (structural ash) and Fe (vegetation ash) ash content was ideal to assess the sublethal effect of both fire ashes on V. vulnificus in the transcriptomic analysis. This concentration of structural and vegetation ash resulted in a decrease in the bacterial growth rate. However, the bacteria were able to proliferate, suggesting a sublethal effect of the fire ashes and a potential bacterial stress response. From an environmental perspective, while studies examining metal concentration in receiving waters following a wildland-urban interface fire are limited, the selected concentrations used in this study are relevant to the concentration of metals found in postfire soils and fire ashes.<sup>64</sup> For example, U.S. Geological Survey (USGS) found elevated amounts of As (up to 140 mg kg<sup>-1</sup>), Pb (up to 344 mg kg<sup>-1</sup>), Cr (up to 354 mg kg<sup>-1</sup>), Cu (up to 1370 mg kg<sup>-1</sup>), and Zn (up to 2800 mg kg<sup>-1</sup>) in collected ash and burned soil samples from southern California forest fire areas during October 2007.65

# 3.2. Wildland-Urban Interface Structural Ash Suppressed Vibrio vulnificus Growth and Upregulated Genes Associated with Antibiotic and Metal Resistance. Vibrio vulnificus growth was suppressed by the presence of the A24 structural ash containing high concentrations of Cr, Cu, and As (Figure 2), resulting in an 82% decrease in the bacterial growth rate for the structural ash cultures (0.0323) compared to the no-ash control cultures (0.1838). Analysis of dissolved metals confirmed high dissolved Cr, Cu, and As concentrations in the control media containing structural ash, and the concentrations remained nearly constant throughout the exposure time (Figure S3). These results indicated that the dissolved metal concentration reached equilibrium prior to the start of the exposure and that V. vulnificus were exposed to the same form (e.g., dissolved vs particulate) of the metal throughout the entire exposure. In the presence of *V. vulnificus*, the experimental exposure conditions reflected a slight decrease in concentrations over time, which can be attributed to bacterial metal uptake or metal sorption to other particulates, or a combination of both mechanisms (Figure S3). Bacterial exposure to heavy metals can modulate their growth, physiology, cellular viability, and even biofilm formation. 66,67 A recent study has shown that simultaneous exposure to multiple heavy metals can result in a lower bacterial growth rate and growth yield as compared to individual metal exposures and result in a stress response different from the individual metal responses.<sup>67</sup> Studies examining the impacts of mixed metal exposure on Vibrio are limited, but studies where Vibrio isolates have been exposed to individual metals showed tolerance to Cr (0.4–3.2 g $m L^{-1}$ ), Cu (0.5–3.2 g $m L^{-1}$ ), and other heavy metals. <sup>67–69</sup> A previous study where Vibrio fischeri was exposed to Zn, Cu, and Cd showed that mixed metal exposures could have synergistic or

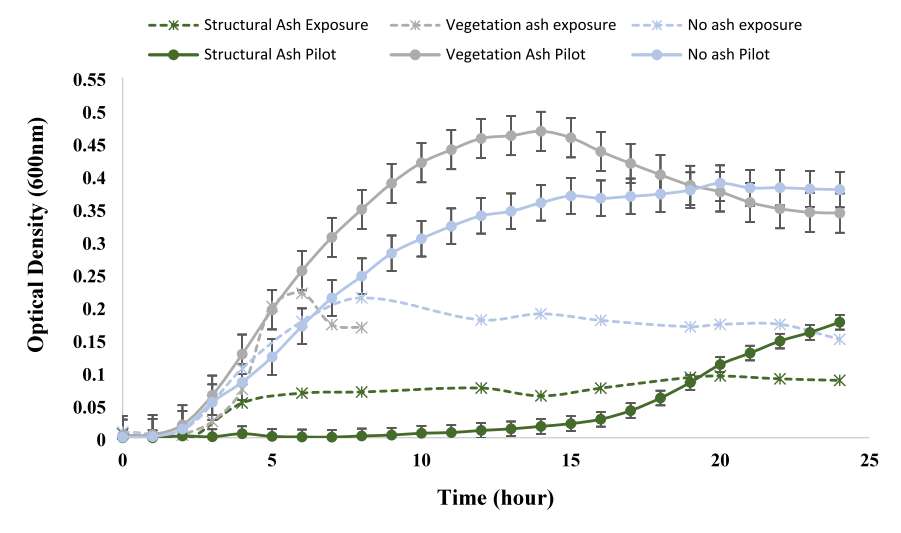


**Figure 2.** Bacterial growth of *V. vulnificus* ATCC 27562 in modified seawater yeast extract containing wildland-urban interface fire ashes. The exposure of *V. vulnificus* ATCC 27562 to two types of fire ashes showed enhanced bacterial growth in the vegetation ashes with a high iron content (gray lines) and suppressed growth in the structural ashes containing copper, arsenic, and chromium (green lines). The control condition, no ashes, is represented by the blue lines. The solid lines represent a pilot study where *V. vulnificus* was grown in experimental conditions in a 96-well plate for 24 h. The dashed lines represent the bacterial growth during the transcriptomic exposure study, where the optical density was measured every 2 h for the structural ash and hourly for the vegetation due to the difference in toxicity determined by the dose—response analysis.

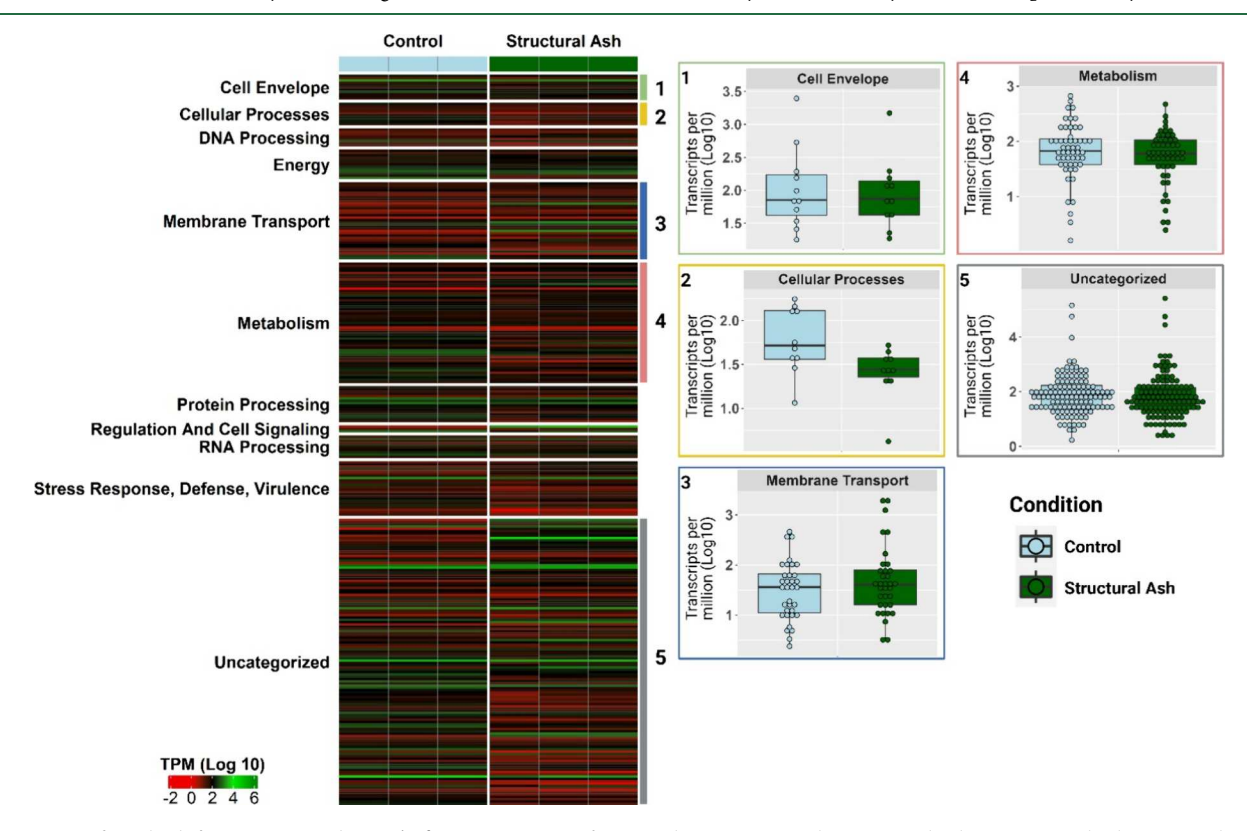


Figure 3. Significantly different expressed V. vulnificus genes across functional categories in the structural ash exposure. The heat map shows the transcripts per million of V. vulnificus significantly different expressed genes (FDR-adjusted p-value of  $\leq$ 0.05) in the structural ash condition as compared with the control (no ash). The box plot shows functional categories with major expression differences between the control and experimental conditions. Blue represents the control condition, and green represents the structural ash experimental condition.

antagonistic effects on the growth depending on the combined metals.  $^{70}$ 

To examine the sublethal effects of wildfire ashes and their metal composition on *V. vulnificus* gene expression, an RNA-seq analysis was performed to identify genes and mechanisms involved in the stress response to the exposure. The transcriptomic profile was examined at the 8 h time point in

the structural ash cultures to minimize the effect of the growth stage-dependent changes in gene expression. Approximately 16.6 to 28 million total reads per replicate (Table S2) were annotated using the *V. vulnificus* NBRC 15645 reference genome in the BV-BRC analysis tool. A total of 4,427 open reading frames (ORFs) were identified, and transcript abundances were compared between conditions. As compared

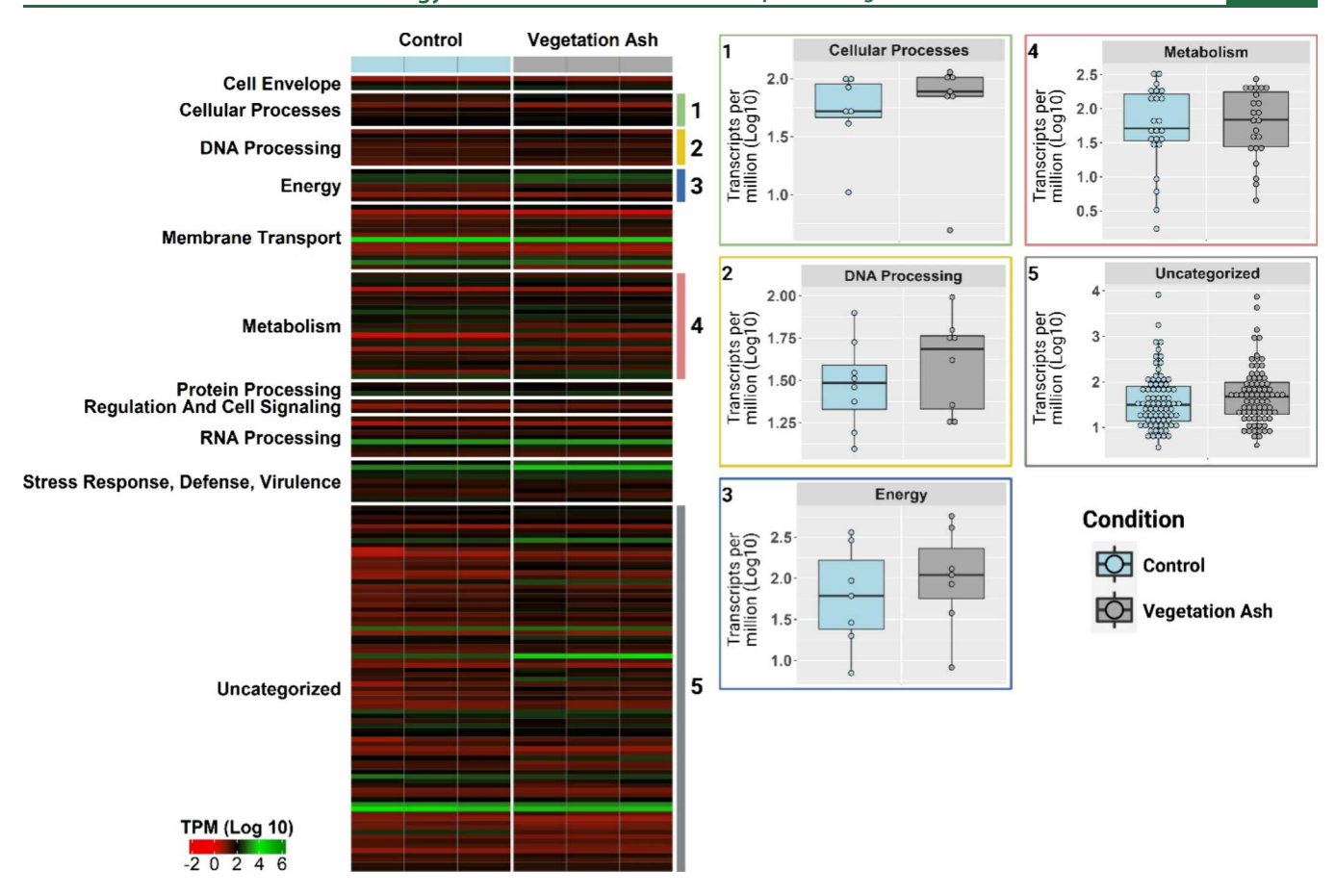
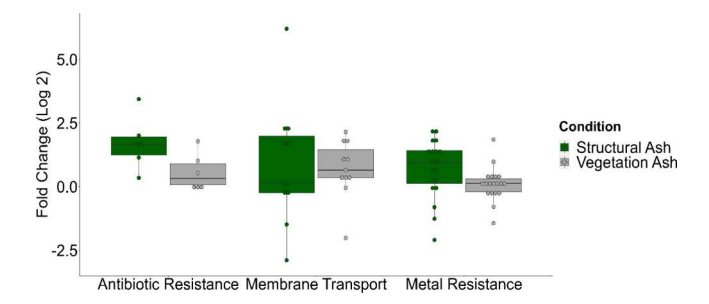


Figure 4. Significantly different expressed *Vibrio vulnificus* genes across functional categories in the vegetation ash exposure. The heat map shows the transcripts per million of *V. vulnificus* significantly different expressed genes (FDR-adjusted p-value of  $\leq$ 0.05) in the vegetation ash conditions as compared with the control (no ash). The box plot shows functional categories with major expression differences between the control and experimental conditions. Blue represents the control condition, and gray represents the vegetation ash experimental condition.



**Figure 5.** Fold change of *V. vulnificus* genes related to metal and antibiotic resistance in structural ash and vegetation ash exposure. Box plots represent the fold change of *V. vulnificus* genes related to antibiotic and metal resistance when exposed to WUI fire ash as compared to the no-ash control. The green color represents the response to structural ash, and the gray color represents the response to vegetation ash.

to the control without ashes, exposure to structural ash resulted in significantly different expression of 278 genes (183 upregulated and 95 downregulated [FDR-adjusted p-value of  $\leq$ 0.05; fold change Log2  $\geq$  |1|]). The Log2 fold change in TPM for the structural ash exposure at 8 h varied between 1.00 to 10.7 for upregulated genes and from -1.00 to -5.77 for downregulated genes. A complete list of significant differentially expressed genes in V. vulnificus exposed to structural ash can be found in Table S5. The principal component analysis (PCA) indicated that the global expression profile

differs between exposure conditions and shows similarity among the biological replicates (Figure S4). The first component (PC1) explained 95.0% of the variation, and the second component (PC2) explained 4.6%. The transcriptomic analysis revealed a consistent differential expression in genes related to the cell envelope, cellular process, and membrane transport functional categories, as shown in Figure 3. The exposure of V. vulnificus to structural ash at environmentally relevant concentrations resulted in upregulated genes and mechanisms related to metal resistance and multidrug efflux pump systems, suggesting a possible coresistance for both metal and antibiotic resistance as an adaptative stress response to the dissolved metals in the ash experimental condition (Table S6). No significant changes in Vibrio genes related to PAH degradation (e.g., dioxygenase genes) were observed, suggesting minimal effects from potential ash-associated PAH exposure.

Cu is an essential trace metal that is used as a cofactor in various proteins due to its redox potential and is involved in metabolic functions such as electron transport and denitrification. High concentrations of Cu can be highly toxic, but many Gram-negative bacteria have regulatory mechanisms that can recognize changes in Cu concentration and maintain a balance that allows essential biochemical processes while preventing the accumulation of toxic levels. This study showed that *V. vulnificus* exposure to excessive Cu concentrations generated by the structural ash dissolved metals triggers a *V. vulnificus* copper response, where *cueR* (figl

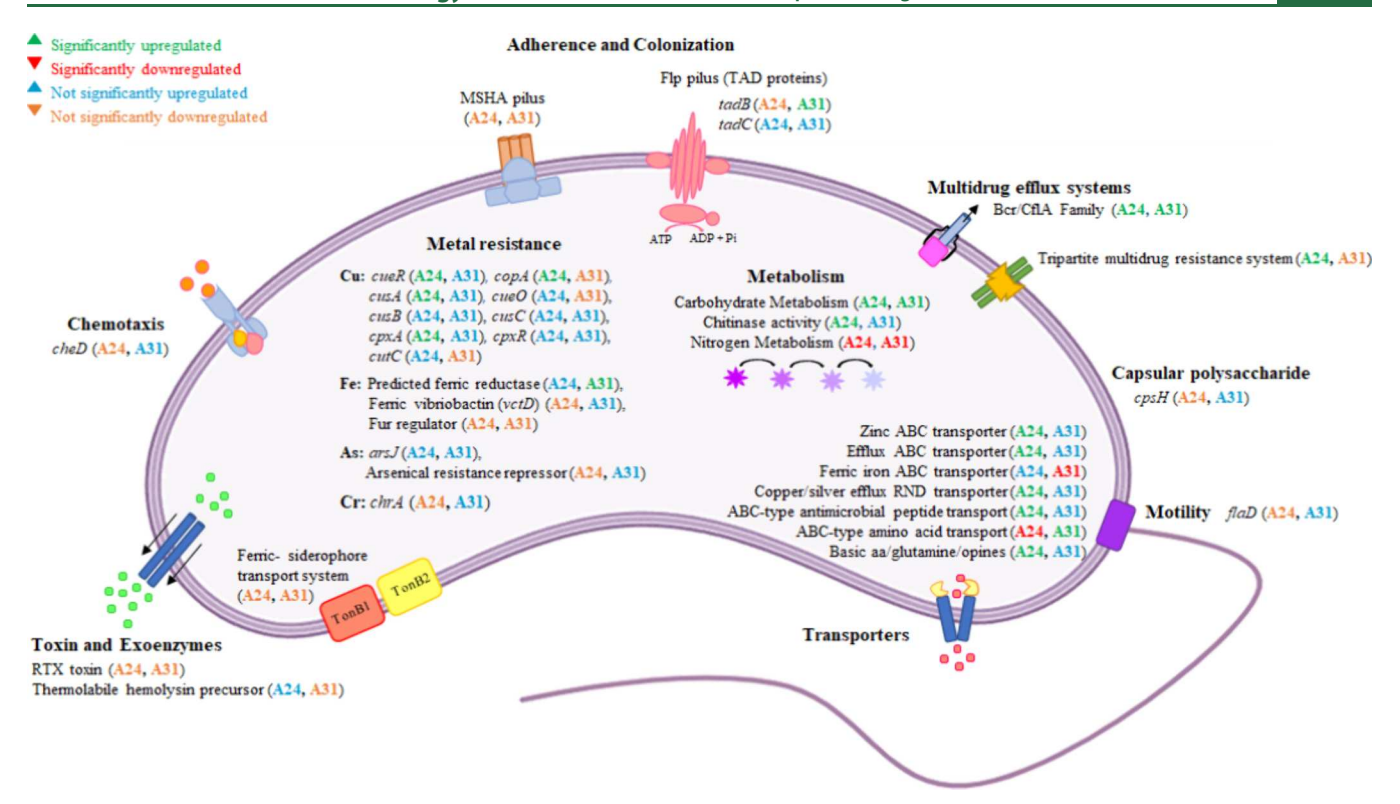


Figure 6. Conceptual model of altered *Vibrio vulnificus* gene expression or pathways as a response to wildland-urban interface fire ash (A24 structural ash and A31 vegetation ash). This conceptual model summarizes the notable *V. vulnificus* expressed genes in the bacterial response to the WUI fire ash exposures, as compared with the no-ash control. A24 represents the response to structural ash, and A31 represents the response to vegetation ash. The text color indicated if the gene or pathway was upregulated or downregulated on the basis of the no-ash control and if the expression was significantly different from the control. The green and red colors represent significantly upregulated and significantly downregulated genes, respectively. The blue and orange colors represent upregulated and downregulated genes that are not significantly different compared to the control, respectively.

1219061.29.peg.1324, copper resistance transcriptional regulator, fold change Log2 = 1.89) activates the expression of Cu homeostasis genes. cueR drives the expression of the copper translocating P-type ATPase (figl1219061.29.peg.2177, copA) that exports Cu(I) from the cytoplasm to the periplasm and where a multicopper oxidase (figl1219061.29.peg.2867, cueO) converts Cu(I) to the less toxic Cu(II) form. The upregulation of cusA (fig|1219061.29.peg.694, fold change Log2 = 1.40) was also observed, suggesting that the cusCFBA system extrudes Cu from the periplasm. These copper tolerance mechanisms have been well-documented in Escherichia coli, Vibrio alginolyticus, Vibrio cholerae (V. cholera), and other Gram-negative bacteria. 76-78 Transcriptomic profiles also showed an upregulation of the cpxA (fig|1219061.29.peg.3114) and cpxR (fig|1219061.29.peg.3115) genes, suggesting that the Cu levels are toxic to the cell. Cu toxicity can be reflected in the cell envelope when the periplasmic Cu(I) inhibits protein maturation by binding to a conserved acyl-accepting Nterminal cysteine residue. A cell envelope stress response is coordinated by the two-component regulator system, cpxAR, to adapt to these high Cu levels. 79 Briefly, cpxA detects the accumulation of the outer membrane lipoproteins and regulates the expression of cpxR, repressing the coppersensitive lipoprotein biosynthesis and inducing the production of maturation enzymes. 80,81 Cpx response has been described as a mechanism in *V. cholera* to mediate adaptation to envelope perturbations caused by toxic compounds and iron depletion. Another gene that was expressed during the structural ash exposure was cutC (figl1219061.29.peg.2356), which has been

documented to be involved in maintaining Cu homeostasis in bacteria.  $^{83-85}$ 

The *V. vulnificus* transcriptomic profile also suggested an adaptive response to increased arsenic by upregulating the expression of the *arsJ* gene (figl1219061.29.peg.3025; fold change Log2 = 2.13), which encodes a major facilitator superfamily (MSF)-type efflux pump for 1-arseno-3-phosphoglycerate (1As3PGA). Chen et al. proposed a response mechanism where intracellular pentavalent arsenate is converted to 1As3PGA by the glyceraldehyde-3-phosphate dehydrogenase enzyme and extruded from the cell by *arsJ*, conferring arsenic resistance. A recent study proposed a new mechanism in *V. cholerae* for arsenate detoxification, suggesting that 1As3PG is dissociated by a putative uncharacterized phosphatase (*varH*) to enable the extrusion of free arsenate through ArsJ. The suggesting that 1Ars3PG is dissociated by a putative uncharacterized phosphatase (*varH*) to enable the extrusion of free arsenate through ArsJ. The suggesting that 1Ars3PG is dissociated by a putative uncharacterized phosphatase (*varH*) to enable the extrusion of free arsenate through ArsJ. The suggesting that 1Ars3PG is dissociated by a putative uncharacterized phosphatase (*varH*) to enable the extrusion of free arsenate through ArsJ.

Another trace metal present during the structural ash exposure was Cr, and the transcriptomic analysis showed downregulation of the chromate-resistance determinant, *chrA*, which encodes a chromate transport protein. While *chrA* expression was suppressed, it is possible that other mechanisms, such as ATP-binding cassette (ABC) transporters, may contribute to chromate efflux from the cytoplasm, aiding in Cr resistance. For instance, exposure to structural ash increased the expression of genes related to membrane transport solute binding protein-dependent systems, particularly ABC transporters (figl1219061.29.peg.2925, figl 1219061.29.peg.3992, and figl1219061.29.peg.2089). ABC transporters are crucial for Gram-negative bacteria as they

facilitate the uptake of vital nutrients, transport bacterial products, and contribute to pathogenicity. They also possess the unique ability to translocate various substrates, from metal ions to proteins including xenobiotics, and can act as importers or exporters. 94,95

Furthermore, multidrug efflux system components were upregulated, particularly the Bcr/CflA family multidrug resistance transporter (fig|1219061.29.peg.888 and fig| 1219061.29.peg.4130) and tripartite multidrug resistance system (fig|1219061.29.peg.759). Pathogenic bacteria use multidrug efflux pumps to transport various molecules, including antibiotics, into and out of the cell. This mechanism reduces intracellular metal concentrations and plays a significant role in colonization and dissemination during host infection and allows bacteria to extrude innate host defenses. Studies have shown that the Bcr/CflA family transporter can confer resistance to chloramphenicol, florfenicol, and bicyclomycin by actively transporting these compounds out of the cell. A putative multidrug efflux pump (EmrD) that shared homology with the Bcr/CflA subfamily has also been identified in *V. cholerae*.

Overall, the pattern of upregulated genes suggests that exposure to structural ash such as A24 ash can trigger a metal and antibiotic coselection response in V. vulnificus. This coselection can occur when both metal and antibiotic resistance genes are present in the bacterial genome (coresistance) or when a singular mechanism can confer resistance to different compounds, for example, certain efflux pumps (cross-resistance/coregulation). 101-104 Previous studies have suggested that exposure to heavy metals can play a role in the coselection and proliferation of antibiotic-resistant bacteria. 105-107 Recent studies have indicated that subinhibitory concentrations of heavy metals in the environment, including copper, enhance antibiotic resistance by inducing mutagenesis in bacteria. 108,109 Cu exposure also appears to increase the potential for horizontal transfer of antibioticresistant genes in the environment. 110,111

3.3. Wildland-Urban Interface Vegetation Ash Enhanced Vibrio vulnificus Growth and Upregulated Gene Associated with Metabolism. The mobilization of wildfire ashes by wind or water into the surrounding environments, including the ocean, has been correlated with increases in iron levels. 112,113 In contrast to the structural ash, V. vulnificus growth was enhanced during the vegetation ash exposure where the growth rate increased by 46% (0.2692) as compared to the control condition (no ash, 0.1838) as shown in Figure 2. It is important to mention that this increase in growth occurs in the sublethal metal concentrations, and the response can change depending on the fire ash concentration. The dissolved metal analysis showed that dissolved Fe concentrations were below the detection limit for vegetation ash in the presence and absence of V. vulnificus (Figure S3). In this case, while Fe was present in all exposure studies, it formed insoluble aggregates with media components and was removed during the ultrafiltration step of sample processing. Thus, during the vegetation ash experiments, V. vulnificus is likely exposed more to Fe aggregates as compared to dissolved Fe. Fe availability is considered a crucial factor in V. vulnificus growth and survival during human host infections and constitutes the major bacteriostatic limitation in human serum. 114-116

The transcriptomic profile was examined at the 3 h time point, representing the exponential growth phase in the vegetation ash conditions, to minimize the effect of the growth stage-dependent changes in gene expression. A total of 48.3 to 101.6 million sequences per replicate were annotated to the reference genome, resulting in 4427 ORFs (Table S2). The transcript abundances were compared between the exposure to the vegetation ash and without ash resulting in significantly different expression of 132 genes (82 upregulated and 50 downregulated FDR-adjusted p-value of  $\leq 0.05$ ; fold change  $Log2 \ge |1|$ ]). The Log2 fold change in TPM for the vegetation ash exposure varied between 1.00 and 3.39 for upregulated genes and from -1.00 to -3.39 for downregulated genes. Table S7 contains a complete list of significant differentially expressed genes in V. vulnificus exposure to vegetation ash. The difference in the global expression profile between the experimental conditions and the similarity among the biological replicates are represented in Figure S5. The first component (PC1) of the PCA explained 69.8% of the variation, and the second component (PC2) explained 16.2%.

The V. vulnificus transcriptomic profile for vegetation ash exposure exhibited a profile similar to that of the control condition with a slight enrichment in genes related to cellular processes, DNA processing, and energy (Figure 4). The upregulation of genes related to energy and metabolism suggested enhanced growth, and the downregulation of genes related to iron acquisition further confirmed the presence of elevated iron concentration in the vegetation ash exposure conditions (Tables S6 and S7). Iron plays a crucial role in several physiological processes of bacterial growth and pathogenesis and can exist in two forms in the environment: ferrous iron (Fe<sup>2+</sup>) and ferric iron (Fe<sup>3+</sup>).<sup>117</sup> The main ironresponsive transcription factor is Fur (ferric uptake regulator), which regulates cellular iron levels by controlling the transcription of iron acquisition-related genes and maintaining iron homeostasis. 118,119 V. vulnificus gene expression profiles for the vegetation ash exposure showed the downregulation of fur (figl1219061.29.peg.2111), suggesting an iron homeostasis response and the downregulation of the iron acquisitionrelated genes as expected in an iron-replete condition. The Fur regulation under iron excess is supported by the upregulation of a predicted ferric reductase (figl1219061.29.peg.688) and downregulation of ferric iron ABC transporter protein (figl 1219061.29.peg.3478) and outer membrane porin (ompU, figl 1219061.29.peg.3502).

**3.4.** Conceptual Model and Potential Coastal Ecosystem Implications. There is limited knowledge about the impact of fire ashes on microbial communities within estuary and coastal ecosystems. Fire ashes are highly mobile and contain nutrients, toxic metals, and metalloids that can incorporate into the soil, be transported by water or runoff, and be mobilized by smoke and wind compromising human and environmental health. <sup>40,120</sup> Fire ashes reaching estuarine and coastal zones alter nutrient, carbon, and metal concentrations resulting in changes in the coastal microbial community composition and phytoplankton production. <sup>112,121–123</sup>

This study aimed to establish a foundational understanding of the potential repercussions of environmentally relevant concentrations of WUI fire ashes on coastal microbial communities using *V. vulnificus* as a model of an opportunistic bacterial pathogen that is prevalent in many estuarine ecosystems. Overall, the findings indicate that *V. vulnificus* increased coexpression of genes and pathways related to antibiotic and metal resistance as an adaptative response to fire ash exposure (Figure 5), with greater effects observed in the structural ash exposure. Figure 6 provides a conceptual model

elucidating how the different fire ashes altered Vibrio gene expression and the potentially affected genetic pathways. The excess Fe (and possibly other unmeasured components) contained in the vegetation ash enhanced bacterial growth and upregulated the expression of genes related to energy and metabolic pathways, such as carbohydrate metabolism. Conversely, Cu, Cr, and As contained in the structural ash suppressed growth while markedly upregulating genes related to metal and antibiotic resistance. For instance, the structural ash transcriptomic profile reflects the expression of bacterial resistance mechanisms, including homeostasis mechanisms involved in Cu detoxification (copA, cueR, and cusCFBA) and the coexpression of multidrug transport systems and efflux pumps. Interestingly, exposure to both fire ashes (structural and vegetation) led to the upregulation of multidrug resistance transporters of the Bcr/CflA subfamily. Multidrug efflux pumps recognize many compounds and have been shown to be an essential bacterial mechanism for overcoming selective pressures and adapting to diverse environments. Furthermore, they play a critical role in conferring resistance against various antimicrobial classes by reducing their cytosolic concentration through active extrusion. 124

In summary, these findings show that V. vulnificus demonstrates different adaptive responses based on the specific composition of fire ashes. While this laboratory study assessed the effects of structural and vegetation ashes separately, it is crucial to acknowledge that natural conditions in estuarine and coastal ecosystems typically involve mixed ashes from various sources within the wildland-urban interface. The transport and deposition of mixed ashes into ecosystems conducive to Vibrio growth may not only enhance the growth of V. vulnificus but also select for more antibiotic-resistant phenotypes, posing a potential public health risk of exposure to resistant strains in coastal zones. With increasing population, human activities, and abnormal weather events in coastal zones, leading to increased Vibrio-human interactions, the risk may be amplified. Although seafood consumption is not the focus of this study, Vibrio strains with altered virulence profiles can also accumulate in shellfish, potentially causing infections during processing and consumption. While this study provides a foundation of how fire ashes can influence the growth and gene expression profiles of a potential human pathogen, future studies should also consider climate change conditions, different V. vulnificus biotypes, complex microbial community models, individual and complex metals, and the intricacies of the natural system, including food web dynamics, to better define environmental and public health risks related to fire ash-Vibrio interactions.

## ASSOCIATED CONTENT

#### **5** Supporting Information

The Supporting Information is available free of charge at https://pubs.acs.org/doi/10.1021/acs.est.3c08658.

(Figure S1) Total elemental concentrations in the wildland-urban interface wildfire ashes; (Figure S2) graphical methodology of *Vibrio vulnificus* exposure to different wildland-urban interface fire ashes; (Figure S3) dissolved chromium, copper, and arsenic concentrations in modified seawater yeast extract containing wildland-urban interface structural and vegetation ash; (Figure S4) principal component analysis (PCA) plot of the global gene expression profile of *Vibrio vulnificus* exposed

to structural fire ash and the control condition (no ash); (Figure S5) principal component analysis (PCA) plot of the global gene expression profile of *Vibrio vulnificus* exposed to vegetation fire ash and the control condition (no ash) (PDF)

(Table S1) Fire ash amounts and relevant metal concentrations used in the concentration—response analysis; (Table S2) summary of the sequences used for RNA-seq analysis using the BV-BRC analysis tool; (Table S3) summary of TOFWERK ICP-TOF-MS operating conditions; (Table S4) list of monitored isotopes during the dissolved metal concentration analysis; (Table S5) V. vulnificus significantly different expressed genes as a response to structural ash (A24) exposure (FDR-adjusted p-value of ≤0.05); (Table S6) V. vulnificus expressed genes related to metal and antibiotic resistance as a response to WUI fire ash A24 and A31; (Table S7) V. vulnificus significantly different expressed genes as a response to vegetation ash (A31) exposure (FDR-adjusted p-value of ≤0.05) (XLSX)

### AUTHOR INFORMATION

#### **Corresponding Author**

R. Sean Norman — Department of Environmental Health Sciences and NIEHS Center for Oceans and Human Health and Climate Change Interactions, University of South Carolina, Columbia, South Carolina 29208, United States; orcid.org/0000-0003-4766-4376; Email: rsnorman@mailbox.sc.edu

#### **Authors**

Karlen Enid Correa Velez — Department of Environmental Health Sciences and NIEHS Center for Oceans and Human Health and Climate Change Interactions, University of South Carolina, Columbia, South Carolina 29208, United States

Mahbub Alam – Department of Environmental Health Sciences and Center for Environmental Nanoscience and Risk, University of South Carolina, Columbia, South Carolina 29208, United States

Mohammed A. Baalousha – Department of Environmental Health Sciences and Center for Environmental Nanoscience and Risk, University of South Carolina, Columbia, South Carolina 29208, United States; orcid.org/0000-0001-7491-4954

Complete contact information is available at: https://pubs.acs.org/10.1021/acs.est.3c08658

#### Notes

The authors declare no competing financial interest.

#### ACKNOWLEDGMENTS

We thank the NIEHS Center for Oceans and Human Health and Climate Change Interactions at the University of South Carolina (Grant No. P01ES028942) and Dr. Mohammed Baalousha Rapid NSF grant (Grant No. 2101983) for the financial support for this research. We also thank Charles N. Alpers from the U.S. Geological Survey, California Water Science Center, for the collection of the ash samples.

#### REFERENCES

(1) Garcia-Soto, C.; Cheng, L.; Caesar, L.; Schmidtko, S.; Jewett, E. B.; Cheripka, A.; Rigor, I.; Caballero, A.; Chiba, S.; Báez, J. C.;

- Zielinski, T.; Abraham, J. P. An Overview of Ocean Climate Change Indicators: Sea Surface Temperature, Ocean Heat Content, Ocean pH, Dissolved Oxygen Concentration, Arctic Sea Ice Extent, Thickness and Volume, Sea Level and Strength of the AMOC (Atlantic Meridional Overturning Circulation). Frontiers in Marine Science. 2021, 8, No. 642372.
- (2) Cazenave, A.; Dieng, H.; Meyssignac, B.; Von Schuckmann, K.; Decharme, B.; Berthier, E. The rate of sea-level rise. *Nature Climate Change* **2014**, *4*, 358–361.
- (3) Cloern, J. E.; Abreu, P. C.; Carstensen, J.; Chauvaud, L.; Elmgren, R.; Grall, J.; Greening, H.; Johansson, J. O.; Kahru, M.; Sherwood, E. T.; Xu, J.; Yin, K. Human activities and climate variability drive fast-paced change across the world's estuarine-coastal ecosystems. *Global change biology* **2016**, 22 (2), 513–529.
- (4) Day, J. W.; Rybczyk, J. M. Global Change Impacts on the Future of Coastal Systems: Perverse Interactions Among Climate Change, Ecosystem Degradation, Energy Scarcity, and Population. *Coasts and Estuaries* **2019**, 621–639.
- (5) Epstein, P. R. Climate change and emerging infectious diseases. *Microbes and infection* **2001**, 3 (9), 747–754.
- (6) Trinanes, J.; Martinez-Urtaza, J. Future scenarios of risk of *Vibrio* infections in a warming planet: a global mapping study. *Lancet. Planetary health* **2021**, *S* (7), e426–e435.
- (7) Mora, C.; McKenzie, T.; Gaw, I. M.; Dean, J. M.; von Hammerstein, H.; Knudson, T. A.; Setter, R. O.; Smith, C. Z.; Webster, K. M.; Patz, J. A.; Franklin, E. C. Over half of known human pathogenic diseases can be aggravated by climate change. *Nature Climate Change* **2022**, *12* (9), 869–875.
- (8) Baker-Austin, C.; Trinanes, J.; Taylor, N.; Hartnell, R.; Siitonen, A.; Martinez-Urtaza, J. Emerging *Vibrio* risk at high latitudes in response to ocean warming. *Nature Climate Change* **2013**, *3*, 73–77.
- (9) Newton, A.; Kendall, M.; Vugia, D. J.; Henao, O. L.; Mahon, B. E. Increasing rates of vibriosis in the United States, 1996–2010: review of surveillance data from 2 systems. *Clin. Infect. Diseases* **2012**, 54, S391–S395.
- (10) Vezzulli, L.; Colwell, R. R.; Pruzzo, C. Ocean warming and spread of pathogenic vibrios in the aquatic environment. *Microbial ecology* **2013**, *65* (4), 817–825.
- (11) Baker-Austin, C.; Trinanes, J.; Gonzalez-Escalona, N.; Martinez-Urtaza, J. Non-Cholera Vibrios: The Microbial Barometer of Climate Change. *Trends in microbiology* **2017**, 25 (1), 76–84.
- (12) Baker-Austin, C.; Oliver, J. D.; Alam, M.; Ali, A.; Waldor, M. K.; Qadri, F.; Martinez-Urtaza, J. Vibrio spp. infections. Nature reviews. Disease primers 2018, 4 (1), 1.
- (13) Thompson, J. R.; Randa, M. A.; Marcelino, L. A.; Tomita-Mitchell, A.; Lim, E.; Polz, M. F. Diversity and dynamics of a North Atlantic coastal *Vibrio* community. *Applied and environmental microbiology* **2004**, *70* (7), 4103–4110.
- (14) Martinez-Urtaza, J.; Lozano-Leon, A.; Varela-Pet, J.; Trinanes, J.; Pazos, Y.; Garcia-Martin, O. Environmental determinants of the occurrence and distribution of *Vibrio parahaemolyticus* in the rias of Galicia. *Spain. Applied and environmental microbiology* **2008**, 74 (1), 265–274.
- (15) Vezzulli, L.; Pezzati, E.; Moreno, M.; Fabiano, M.; Pane, L.; Pruzzo, C. Benthic ecology of *Vibrio* spp. and pathogenic *Vibrio* species in a coastal Mediterranean environment (La Spezia Gulf, Italy). *Microbial ecology* **2009**, *58* (4), 808–818.
- (16) Wang, X.; Liu, J.; Liang, J.; Sun, H.; Zhang, X. H. Spatiotemporal dynamics of the total and active *Vibrio* spp. populations throughout the Changjiang estuary in China. *Environmental microbiology* **2020**, 22 (10), 4438–4455.
- (17) FAO and WHO. Risk assessment tools for Vibrio parahaemolyticus and Vibrio vulnificus associated with seafood. Microbiological Risk Assessment Series No. 20. Rome, 2020.
- (18) Archer, E. J.; Baker-Austin, C.; Osborn, T. J.; Jones, N. R.; Martínez-Urtaza, J.; Trinanes, J.; Oliver, J. D.; González, F. J. C.; Lake, I. R. Climate warming and increasing *Vibrio vulnificus* infections in North America. *Sci. Rep.* **2023**, *13* (1), 3893.

- (19) Sodders, N.; Stockdale, K.; Baker, K.; Ghanem, A.; Vieth, B.; Harder, T. Notes from the Field: Vibriosis Cases Associated with Flood Waters During and After Hurricane Ian Florida, September-October 2022. MMWR. Morbidity and mortality weekly report 2023, 72 (18), 497–498.
- (20) Brumfield, K. D.; Usmani, M.; Santiago, S.; Singh, K.; Gangwar, M.; Hasan, N. A.; Netherland, M.; Deliz, K.; Angelini, C.; Beatty, N. L.; Huq, A.; Jutla, A. S.; Colwell, R. R.; Vidaver, A. K. Genomic diversity of *Vibrio* spp. and metagenomic analysis of pathogens in Florida Gulf coastal waters following Hurricane Ian. *mBio* 2023, 14 (6), No. e0147623.
- (21) Jones, M. K.; Oliver, J. D. Vibrio vulnificus: disease and pathogenesis. Infection and immunity 2009, 77 (5), 1723-1733.
- (22) Oliver, J. D. The Biology of Vibrio vulnificus. Microbiol. Spectrum 2015, 3 (3), 10 DOI: 10.1128/microbiolspec.VE-0001-2014.
- (23) Eun Rhee, J.; Haeng Rhee, J.; Youl Ryu, P.; Ho Choi, S. Identification of the cadBA operon from *Vibrio vulnificus* and its influence on survival to acid stress. *FEMS Microbiol. Lett.* **2002**, 208 (2), 245–251.
- (24) Pettis, G. S.; Mukerji, A. S. Structure, Function, and Regulation of the Essential Virulence Factor Capsular Polysaccharide of *Vibrio vulnificus*. *International journal of molecular sciences* **2020**, 21 (9), 3259.
- (25) Li, G.; Wang, M. Y. The role of *Vibrio vulnificus* virulence factors and regulators in its infection-induced sepsis. *Folia microbiologica* **2020**, *65* (2), 265–274.
- (26) Bisharat, N.; Bronstein, M.; Korner, M.; Schnitzer, T.; Koton, Y. Transcriptome profiling analysis of *Vibrio vulnificus* during human infection. *Microbiology (Reading)* **2013**, *159* (9), 1878–1887.
- (27) Williams, T. C.; Blackman, E. R.; Morrison, S. S.; Gibas, C. J.; Oliver, J. D. Transcriptome sequencing reveals the virulence and environmental genetic programs of *Vibrio vulnificus* exposed to host and estuarine conditions. *PloS One* **2014**, *9* (12), No. e114376.
- (28) Pajuelo, D.; Hernández-Cabanyero, C.; Sanjuan, E.; Lee, C. T.; Silva-Hernández, F. X.; Hor, L. I.; MacKenzie, S.; Amaro, C. Iron and Fur in the life cycle of the zoonotic pathogen *Vibrio vulnificus*. *Environmental microbiology* **2016**, *18* (11), 4005–4022.
- (29) Hernández-Cabanyero, C.; Lee, C. T.; Tolosa-Enguis, V.; Sanjuán, E.; Pajuelo, D.; Reyes-López, F.; Tort, L.; Amaro, C. Adaptation to host in *Vibrio vulnificus*, a zoonotic pathogen that causes septicemia in fish and humans. *Environmental microbiology* **2019**, *21* (8), 3118–3139.
- (30) Hernández-Cabanyero, C.; Sanjuán, E.; Fouz, B.; Pajuelo, D.; Vallejos-Vidal, E.; Reyes-López, F. E.; Amaro, C. The Effect of the Environmental Temperature on the Adaptation to Host in the Zoonotic Pathogen *Vibrio vulnificus*. Frontiers in microbiology **2020**, 11, 489.
- (31) Phillips, K. E.; Satchell, K. J. Vibrio vulnificus: From Oyster Colonist to Human Pathogen. PLoS pathogens 2017, 13 (1), No. e1006053.
- (32) Correa Velez, K. E.; Norman, R. S. Transcriptomic Analysis Reveals That Municipal Wastewater Effluent Enhances *Vibrio vulnificus* Growth and Virulence Potential. *Frontiers in microbiology* **2021**, *12*, No. 754683.
- (33) Brumfield, K. D.; Chen, A. J.; Gangwar, M.; Usmani, M.; Hasan, N. A.; Jutla, A. S.; Huq, A.; Colwell, R. R.; Semrau, J. D. Environmental Factors Influencing Occurrence of *Vibrio parahaemolyticus* and *Vibrio vulnificus*. *Appl. Environ. Microbiol.* **2023**, 89 (6), No. e0030723.
- (34) López-Pérez, M.; Jayakumar, J. M.; Haro-Moreno, J. M.; Zaragoza-Solas, A.; Reddi, G.; Rodriguez-Valera, F.; Shapiro, O. H.; Alam, M.; Almagro-Moreno, S.; Laub, M. T.; Jensen, P.; Gómez-Consarnau, L. Evolutionary Model of Cluster Divergence of the Emergent Marine Pathogen *Vibrio vulnificus*: From Genotype to Ecotype. *mBio* **2019**, *10* (1), e02852–18.
- (35) López-Pérez, M.; Jayakumar, J. M.; Grant, T. A.; Zaragoza-Solas, A.; Cabello-Yeves, P. J.; Almagro-Moreno, S. Ecological diversification reveals routes of pathogen emergence in endemic

- Vibrio vulnificus populations. Proc. Natl. Acad. Sci. U.S.A. 2021, 118 (40), No. e2103470118.
- (36) Froelich, B. A.; Daines, D. A. In hot water: effects of climate change on *Vibrio*-human interactions. *Environmental Microbiology* **2020**, 22 (10), 4101–4111.
- (37) Moritz, M. A.; Parisien, M. A.; Batllori, E.; Krawchuk, M. A.; Van Dorn, J.; Ganz, D. J.; Hayhoe, K. Climate change and disruptions to global fire activity. *Ecosphere* **2012**, *3* (6), 1–22.
- (38) Bladon, K. D.; Emelko, M. B.; Silins, U.; Stone, M. Wildfire and the Future of Water Supply. *Environ. Sci. Technol.* **2014**, 48 (16), 8936–8943.
- (39) Pausas, J. G.; Keeley, J. E. Wildfires and global change. Frontiers in Ecology and the Environment 2021, 19 (7), 387–395.
- (40) Bodí, M. B.; Martin, D. A.; Balfour, V. N.; Santín, C.; Doerr, S. H.; Pereira, P.; Cerdà, A.; Mataix-Solera, J. Wildland fire ash: Production, composition and eco-hydro-geomorphic effects. *Earth-Science Reviews* **2014**, *130*, 103–127.
- (41) Wasson, S. J.; Linak, W. P.; Gullett, B. K.; King, C. J.; Touati, A.; Huggins, F. E.; Chen, Y.; Shah, N.; Huffman, G. P. Emissions of chromium, copper, arsenic, and PCDDs/Fs from open burning of CCA-treated wood. *Environ. Sci. Technol.* **2005**, *39* (22), 8865–8876.
- (42) Brito, D. Q.; Passos, C. J. S.; Muniz, D. H. F.; Oliveira-Filho, E. C. Aquatic ecotoxicity of ashes from Brazilian savanna wildfires. *Environmental science and pollution research international* **2017**, 24 (24), 19671–19682.
- (43) Radeloff, V. C.; Helmers, D. P.; Kramer, H. A.; Mockrin, M. H.; Alexandre, P. M.; Bar-Massada, A.; Butsic, V.; Hawbaker, T. J.; Martinuzzi, S.; Syphard, A. D.; Stewart, S. I. Rapid growth of the U.S. wildland-urban interface raises wildfire risk. *Proc. Natl. Acad. Sci. U.S.A.* **2018**, *115* (13), 3314–3319.
- (44) Plumlee, G. S.; Morman, S. A.; Meeker, G.; Hoefen, T. M.; Hageman, R. E.; Wolf, R. E. The environmental and medical geochemistry of potentially hazardous materials produced by disasters. *Treatise on Geochemistry* **2014**, *11*, 257–304.
- (45) Alam, M.; Alshehri, T.; Wang, J.; Singerling, S. A.; Alpers, C. N.; Baalousha, M. Identification and quantification of Cr, Cu, and As incidental nanomaterials derived from CCA-treated wood in wildlandurban interface fire ashes. *Journal of hazardous materials* **2023**, 445, No. 130608.
- (46) Solo-Gabriele, H. M.; Townsend, T. G.; Messick, B.; Calitu, V. Characteristics of chromated copper arsenate-treated wood ash. *Journal of hazardous materials* **2002**, *89* (2–3), 213–232.
- (47) de Medeiros Domingos, D.; Scussel, R.; Canever, S. B.; Soares, B. Q.; Angioletto, E.; Bernardin, A. M.; Pich, C. T. Toxicity of fly ash effluent from the combustion of (chromated copper arsenate)-treated wood. *Cleaner Materials* **2022**, *3* (100051), 100051–7.
- (48) Reichelt, J. L.; Baumann, P.; Baumann, L. Study of genetic relationships among marine species of the genera *Beneckea* and *Photobacterium* by means of in vitro DNA/DNA hybridization. *Archives of microbiology* **1976**, *110* (1), 101–120.
- (49) Alshehri, T.; Wang, J.; Singerling, S. A.; Gigault, J.; Webster, J. P.; Matiasek, S. J.; Alpers, C. N.; Baalousha, M. Wildland-urban interface fire ashes as a major source of incidental nanomaterials. *Journal of Hazardous Materials* **2023**, 443 (b), No. 130311.
- (50) Oliver, J. D.; Colwell, R. R. Extractable lipids of gram-negative marine bacteria: phospholipid composition. *J. Bacteriol.* **1973**, 114 (3), 897–908.
- (51) Midani, F. S.; Collins, J.; Britton, R. A.; Silva-Rocha, R. AMiGA: Software for Automated Analysis of Microbial Growth Assays. *mSystems* **2021**, *6* (4), No. e0050821.
- (52) Ritz, C.; Baty, F.; Streibig, J. C.; Gerhard, D. Dose-Response Analysis Using R. PloS one 2015, 10 (12), No. e0146021.
- (53) R Core Team R: A language and environment for statistical computing. R Foundation for Statistical Computing: Vienna, Austria. (2022) https://www.R-project.org/.
- (54) Posit team RStudio: Integrated Development Environment for R. Posit Software: PBC, Boston, MA. (2023) http://www.posit.co/.

- (55) Chen, S.; Zhou, Y.; Chen, Y.; Gu, J. fastp: an ultra-fast all-in-one FASTQ preprocessor. *Bioinformatics (Oxford, England)* **2018**, 34 (17), i884—i890.
- (56) Olson, R. D.; Assaf, R.; Brettin, T.; Conrad, N.; Cucinell, C.; Davis, J. J.; Dempsey, D. M.; Dickerman, A.; Dietrich, E. M.; Kenyon, R. W.; Kuscuoglu, M.; Lefkowitz, E. J.; Lu, J.; Machi, D.; Macken, C.; Mao, C.; Niewiadomska, A.; Nguyen, M.; Olsen, G. J.; Overbeek, J. C.; Parrello, B.; Parrello, V.; Porter, J. S.; Pusch, G. D.; Shukla, M.; Singh, I.; Stewart, L.; Tan, G.; Thomas, C.; VanOeffelen, M.; Vonstein, V.; Wallace, Z. S.; Warren, A. S.; Wattam, A. R.; Xia, F.; Yoo, H.; Zhang, Y.; Zmasek, C. M.; Scheuermann, R. H.; Stevens, R. L. Introducing the Bacterial and Viral Bioinformatics Resource Center (BV-BRC): a resource combining PATRIC, IRD and ViPR. *Nucleic acids research* 2023, *51* (D1), D678–D68.
- (57) Langmead, B.; Salzberg, S. L. Fast gapped-read alignment with Bowtie 2. *Nat. Methods* **2012**, *9* (4), 357–359.
- (58) Love, M. I.; Huber, W.; Anders, S. Moderated estimation of fold change and dispersion for RNA-seq data with DESeq2. *Genome Biol.* **2014**, *15* (12), 550.
- (59) Putri, G. H., Anders, S., Pyl, P. T., Pimanda, J. E., Zanini, F. (2022). Analysing high-throughput sequencing data in Python with HTSeq 2.0. Bioinformatics: (Oxford, England), 38(10), 2943–2945
- (60) Gu, Z.; Eils, R.; Schlesner, M. Complex heatmaps reveal patterns and correlations in multidimensional genomic data. *Bioinformatics (Oxford, England)* **2016**, 32 (18), 2847–2849.
- (61) Gu, Z. Complex heatmap visualization. IMeta 2022, 1 (3), No. e43.
- (62) Wickham, H. ggplot2: Elegant Graphics for Data Analysis. Springer-Verlag: New York. (2016) ISBN 978-3-319-24277-4, https://ggplot2.tidyverse.org.
- (63) Vu, V. Q. ggbiplot: A ggplot2 based biplot. R package version 2011, 0, 55, http://github.com/vqv/ggbiplot
- (64) Abraham, J.; Dowling, K.; Florentine, S. The Unquantified Risk of Post-Fire Metal Concentration in Soil: a Review. *Water Air Soil Pollut.* **2017**, 228 (175), 1–33.
- (65) Plumlee, G. S., Martin, D. A., Hoefen, T., Kokaly, R. F., Hageman, P., Eckberg, A., Meeker, G. P., Adams, M., Anthony, M., Lamothe, P. J. (2007). Preliminary analytical results for ash and burned soils from the October 2007 southern California wildfires. *US Geological Survey*, doi.org/10.3133/ofr20071407. Open Report No. 2007–1407
- (66) Syed, A.; Zeyad, M. T.; Shahid, M.; Elgorban, A. M.; Alkhulaifi, M. M.; Ansari, I. A. Heavy Metals Induced Modulations in Growth, Physiology, Cellular Viability, and Biofilm Formation of an Identified Bacterial Isolate. *ACS omega* **2021**, *6* (38), 25076–25088.
- (67) Goff, J. L.; Chen, Y.; Thorgersen, M. P.; Hoang, L. T.; Poole, F. L., 2nd; Szink, E. G.; Siuzdak, G.; Petzold, C. J.; Adams, M. W. W. Mixed heavy metal stress induces global iron starvation response. *ISME journal* **2023**, *17* (3), 382–392.
- (68) He, Y.; Jin, L.; Sun, F.; Hu, Q.; Chen, L. Antibiotic and heavymetal resistance of *Vibrio parahaemolyticus* isolated from fresh shrimps in Shanghai fish markets, China. *Environmental science and pollution research international* **2016**, 23 (15), 15033–15040.
- (69) Xu, M.; Wu, J.; Chen, L. Virulence, antimicrobial and heavy metal tolerance, and genetic diversity of *Vibrio cholerae* recovered from commonly consumed freshwater fish. *Environmental science and pollution research international* **2019**, 26 (26), 27338.
- (70) Preston, S.; Coad, N.; Townend, J.; Killham, K.; Paton, G. I. Biosensing the acute toxicity of metal interactions: Are they additive, synergistic, or antagonistic? *Environ. Toxicol. Chem.* **2000**, *19* (3), 775–780.
- (71) Dupont, C. L.; Grass, G.; Rensing, C. Copper toxicity and the origin of bacterial resistance-new insights and applications. *Metallomics: integrated biometal science* **2011**, 3 (11), 1109–1118.
- (72) Singh, K.; Senadheera, D. B.; Cvitkovitch, D. G. An intimate link: two-component signal transduction systems and metal transport systems in bacteria. *Future microbiology* **2014**, *9* (11), 1283–1293.
- (73) Vanhove, A. S.; Rubio, T. P.; Nguyen, A. N.; Lemire, A.; Roche, D.; Nicod, J.; Vergnes, A.; Poirier, A. C.; Disconzi, E.; Bachère, E.; Le

- Roux, F.; Jacq, A.; Charrière, G. M.; Destoumieux-Garzón, D. Copper homeostasis at the host vibrio interface: lessons from intracellular vibrio transcriptomics. *Environmental microbiology* **2016**, *18* (3), 875–888.
- (74) Bondarczuk, K.; Piotrowska-Seget, Z. Molecular basis of active copper resistance mechanisms in Gram-negative bacteria. *Cell biology and toxicology* **2013**, 29 (6), 397–405.
- (75) Giachino, A.; Waldron, K. J. Copper tolerance in bacteria requires the activation of multiple accessory pathways. *Molecular microbiology* **2020**, *114* (3), 377–390.
- (76) Hyre, A.; Casanova-Hampton, K.; Subashchandrabose, S. Copper Homeostatic Mechanisms and Their Role in the Virulence of *Escherichia coli* and *Salmonella enterica*. *EcoSal Plus* **2021**, 9 (2), No. eESP00142020.
- (77) He, R.; Zuo, Y.; Zhao, L.; Ma, Y.; Yan, Q.; Huang, L. Copper stress by nutritional immunity activates the CusS-CusR two-component system that contributes to *Vibrio alginolyticus* anti-host response but affects virulence-related properties. *Aquaculture* **2021**, 532, No. 736012.
- (78) Marrero, K.; Sánchez, A.; González, L. J.; Ledón, T.; Rodríguez-Ulloa, A.; Castellanos-Serra, L.; Pérez, C.; Fando, R. Periplasmic proteins encoded by VCA0261–0260 and VC2216 genes together with copA and cueR products are required for copper tolerance but not for virulence in *Vibrio cholerae*. *Microbiology* **2012**, *158* (Pt 8), 2005–2016.
- (79) May, K. L.; Lehman, K. M.; Mitchell, A. M.; Grabowicz, M.; Hadjifrangiskou, M.; Hultgren, S. J. A Stress Response Monitoring Lipoprotein Trafficking to the Outer Membrane. *mBio* **2019**, *10* (3), e00618–19.
- (80) Raivio, T. L. Everything old is new again: An update on current research on the Cpx envelope stress response. *Biochimica et Biophysica Acta (BBA) Molecular Cell Research* **2014**, *1843* (8), 1529–1541.
- (81) Mitchell, A. M.; Silhavy, T. J. Envelope stress responses: balancing damage repair and toxicity. *Nature reviews. Microbiology* **2019**, *17* (7), 417–428.
- (82) Acosta, N.; Pukatzki, S.; Raivio, T. L. The *Vibrio cholerae* Cpx envelope stress response senses and mediates adaptation to low iron. *J. Bacteriol.* **2015**, *197* (2), *262*–*276*.
- (83) Rensing, C.; Grass, G. *Escherichia coli* mechanisms of copper homeostasis in a changing environment. *FEMS microbiology reviews* **2003**, 27 (2–3), 197–213.
- (84) Latorre, M.; Olivares, F.; Reyes-Jara, A.; López, G.; González, M. CutC is induced late during copper exposure and can modify intracellular copper content in *Enterococcus faecalis*. *Biochemical and biophysical research communications* **2011**, 406 (4), 633–637.
- (85) Ge, Q.; Zhu, X.; Cobine, P. A.; De La Fuente, L. The Copper-Binding Protein CutC Is Involved in Copper Homeostasis and Affects Virulence in the Xylem-Limited Pathogen Xylella fastidiosa. *Phytopathology* **2022**, *112* (8), 1620–1629.
- (86) Chen, J.; Yoshinaga, M.; Garbinski, L. D.; Rosen, B. P. Synergistic interaction of glyceraldehydes-3-phosphate dehydrogenase and ArsJ, a novel organoarsenical efflux permease, confers arsenate resistance. *Molecular microbiology* **2016**, *100* (6), 945–953.
- (87) Bueno, E.; Pinedo, V.; Shinde, D. D.; Mateus, A.; Typas, A.; Savitski, M. M.; Thomas, V. C.; Cava, F.; Roe, A. J.; Ruby, E. G. Transient Glycolytic Complexation of Arsenate Enhances Resistance in the Enteropathogen *Vibrio cholerae. mBio* **2022**, *13* (5), No. e0165422.
- (88) Viti, C.; Marchi, E.; Decorosi, F.; Giovannetti, L. Molecular mechanisms of Cr(VI) resistance in bacteria and fungi. *FEMS microbiology reviews* **2014**, 38 (4), 633–659.
- (89) Chen, J.; Tian, Y. Hexavalent chromium reducing bacteria: mechanism of reduction and characteristics. *Environmental science and pollution research international* **2021**, 28 (17), 20981–20997.
- (90) Garmory, H. S.; Titball, R. W. ATP-binding cassette transporters are targets for the development of antibacterial vaccines and therapies. *Infection and immunity* **2004**, 72 (12), 6757–6763.
- (91) Sheng, Y.; Fan, F.; Jensen, O.; Zhong, Z.; Kan, B.; Wang, H.; Zhu, J. Dual Zinc Transporter Systems in Vibrio cholerae Promote

- Competitive Advantages over Gut Microbiome. *Infection and immunity* **2015**, 83 (10), 3902–3908.
- (92) Tanaka, K. J.; Song, S.; Mason, K.; Pinkett, H. W. Selective substrate uptake: The role of ATP-binding cassette (ABC) importers in pathogenesis. *Biochimica et biophysica acta. Biomembranes* **2018**, 1860 (4), 868–877.
- (93) Akhtar, A. A.; Turner, D. P. The role of bacterial ATP-binding cassette (ABC) transporters in pathogenesis and virulence: Therapeutic and vaccine potential. *Microbial pathogenesis* **2022**, 171, No. 105734.
- (94) Rees, D. C.; Johnson, E.; Lewinson, O. ABC transporters: the power to change. *Nature reviews. Molecular cell biology* **2009**, *10* (3), 218–227.
- (95) Eitinger, T.; Rodionov, D. A.; Grote, M.; Schneider, E. Canonical and ECF-type ATP-binding cassette importers in prokaryotes: diversity in modular organization and cellular functions. *FEMS microbiology reviews* **2011**, 35 (1), 3–67.
- (96) Du, D.; Wang-Kan, X.; Neuberger, A.; van Veen, H. W.; Pos, K. M.; Piddock, L. J. V.; Luisi, B. F. Multidrug efflux pumps: structure, function, and regulation. *Nature reviews. Microbiology* **2018**, *16* (9), 523–539.
- (97) Bissonnette, L.; Champetier, S.; Buisson, J. P.; Roy, P. H. Characterization of the nonenzymatic chloramphenicol resistance (cmlA) gene of the In4 integron of Tn1696: similarity of the product to transmembrane transport proteins. *Journal of bacteriology* **1991**, *173* (14), 4493–4502.
- (98) Braibant, M.; Chevalier, J.; Chaslus-Dancla, E.; Pagès, J. M.; Cloeckaert, A. Structural and functional study of the phenicol-specific efflux pump FloR belonging to the major facilitator superfamily. *Antimicrob. Agents Chemother.* **2005**, *49* (7), 2965–2971.
- (99) Bentley, J.; Hyatt, L. S.; Ainley, K.; Parish, J. H.; Herbert, R. B.; White, G. R. Cloning and sequence analysis of an *Escherichia coli* gene conferring bicyclomycin resistance. *Gene* **1993**, *127* (1), 117–120.
- (100) Smith, K. P.; Kumar, S.; Varela, M. F. Identification, cloning, and functional characterization of EmrD-3, a putative multidrug efflux pump of the major facilitator superfamily from *Vibrio cholerae* O395. *Archives of microbiology* **2009**, *191* (12), 903–911.
- (101) Baker-Austin, C.; Wright, M. S.; Stepanauskas, R.; McArthur, J. V. Co-selection of antibiotic and metal resistance. *Trends in microbiology* **2006**, *14* (4), 176–182.
- (102) Pal, C.; Bengtsson-Palme, J.; Kristiansson, E.; Larsson, D. G. J. Co-occurrence of resistance genes to antibiotics, biocides and metals reveals novel insights into their co-selection potential. *BMC genomics* **2015**, *16*, 964.
- (103) Pal, C.; Asiani, K.; Arya, S.; Rensing, C.; Stekel, D. J.; Larsson, D. G. J.; Hobman, J. L. Metal Resistance and Its Association with Antibiotic Resistance. *Advances in microbial physiology* **2017**, *70*, 261–313.
- (104) Vats, P.; Kaur, U. J.; Rishi, P. Heavy metal-induced selection and proliferation of antibiotic resistance: A review. *Journal of applied microbiology* **2022**, 132 (6), 4058–4076.
- (105) Bhattacharya, M.; Choudhury, P.; Kumar, R. Antibiotic- and metal-resistant strains of *Vibrio parahaemolyticus* isolated from shrimps. *Microbial Drug Resistance* **2000**, *6* (2), 171–172.
- (106) Pathak, S. P.; Gopal, K. Occurrence of antibiotic and metal resistance in bacteria from organs of river fish. *Environmental research* **2005**, 98 (1), 100–103.
- (107) Peltier, E.; Vincent, J.; Finn, C.; Graham, D. W. Zinc-induced antibiotic resistance in activated sludge bioreactors. *Water research* **2010**, *44* (13), 3829–3836.
- (108) Li, X.; Gu, A. Z.; Zhang, Y.; Xie, B.; Li, D.; Chen, J. Sub-lethal concentrations of heavy metals induce antibiotic resistance via mutagenesis. *Journal of hazardous materials* **2019**, 369, 9–16.
- (109) Li, J.; Phulpoto, I. A.; Zhang, G.; Yu, Z. Acceleration of emergence of *E. coli* antibiotic resistance in a simulated sublethal concentration of copper and tetracycline co-contaminated environment. *AMB Express* **2021**, *11* (1), 14.
- (110) Zhang, Y.; Gu, A. Z.; Cen, T.; Li, X.; He, M.; Li, D.; Chen, J. Sub-inhibitory concentrations of heavy metals facilitate the horizontal

- transfer of plasmid-mediated antibiotic resistance genes in water environment. *Environmental pollution (Barking, Essex: 1987)* **2018**, 237, 74–82.
- (111) Zhang, S.; Wang, Y.; Song, H.; Lu, J.; Yuan, Z.; Guo, J. Copper nanoparticles and copper ions promote horizontal transfer of plasmid-mediated multi-antibiotic resistance genes across bacterial genera. *Environ. Int.* **2019**, 129, 478–487.
- (112) Tang, W.; Llort, J.; Weis, J.; Perron, M. M. G.; Basart, S.; Li, Z.; Sathyendranath, S.; Jackson, T.; Sanz Rodriguez, E.; Proemse, B. C.; Bowie, A. R.; Schallenberg, C.; Strutton, P. G.; Matear, R.; Cassar, N. Widespread phytoplankton blooms triggered by 2019–2020 Australian wildfires. *Nature* 2021, 597 (7876), 370–375.
- (113) Rust, A. J.; Roberts, S.; Eskelson, M.; Randell, J.; Hogue, T. S. Forest fire mobilization and uptake of metals by biota temporarily exacerbates impacts of legacy mining. *Science of the total environment* **2022**, 832, No. 155034.
- (114) Wright, A. C.; Simpson, L. M.; Oliver, J. D. Role of iron in the pathogenesis of *Vibrio vulnificus* infections. *Infection and immunity* **1981**, 34 (2), 503–507.
- (115) Bogard, R. W.; Oliver, J. D. Role of iron in human serum resistance of the clinical and environmental *Vibrio vulnificus* genotypes. *Applied and environmental microbiology* **2007**, 73 (23), 7501–7505.
- (116) Kim, H. Y.; Ayrapetyan, M.; Oliver, J. D. Survival of *Vibrio vulnificus* genotypes in male and female serum, and production of siderophores in human serum and seawater. *Foodborne pathogens and disease* **2014**, *11* (2), 119–125.
- (117) Frawley, E. R.; Fang, F. C. The ins and outs of bacterial iron metabolism. *Molecular microbiology* **2014**, *93* (4), *609*–*616*.
- (118) Hantke, K. Iron and metal regulation in bacteria. Curr. Opin. Microbiol. 2001, 4 (2), 172–177.
- (119) Andrews, S. C.; Robinson, A. K.; Rodríguez-Quiñones, F. Bacterial iron homeostasis. *FEMS microbiology reviews* **2003**, 27 (2–3), 215–237.
- (120) Sánchez-García, C.; Santín, C.; Neris, J.; Sigmund, G.; Otero, X.; Manley, J.; González-Rodríguez, G.; Belcher, C.; Cerdà, A.; Marcotte, A.; Murphy, S.; Rhoades, C.; Sheridan, G.; Strydom, T.; Robichaud, P.; Doerr, S. Chemical characteristics of wildfire ash across the globe and their environmental and socio-economic implications. *Environ. Int.* 2023, 178, No. 108065.
- (121) Barros, T. L.; Bracewell, S. A.; Mayer-Pinto, M.; Dafforn, K. A.; Simpson, S. L.; Farrell, M.; Johnston, E. L. Wildfires cause rapid changes to estuarine benthic habitat. *Environmental pollution (Barking, Essex: 1987)* **2022**, *308*, No. 119571.
- (122) Liu, D.; Zhou, C.; Keesing, J. K.; Serrano, O.; Werner, A.; Fang, Y.; Chen, Y.; Masque, P.; Kinloch, J.; Sadekov, A.; Du, Y. Wildfires enhance phytoplankton production in tropical oceans. *Nat. Commun.* **2022**, *13* (1), 1348.
- (123) Ardyna, M.; Hamilton, D. S.; Harmel, T.; Lacour, L.; Bernstein, D. N.; Laliberté, J.; Horvat, C.; Laxenaire, R.; Mills, M. M.; van Dijken, G.; Polyakov, I.; Claustre, H.; Mahowald, N.; Arrigo, K. R. Wildfire aerosol deposition likely amplified a summertime Arctic phytoplankton bloom. *Commun. Earth Environ.* **2022**, *3* (201), 1–8.
- (124) Henderson, P. J. F.; Maher, C.; Elbourne, L. D. H.; Eijkelkamp, B. A.; Paulsen, I. T.; Hassan, K. A. Physiological Functions of Bacterial "Multidrug" Efflux Pumps. *Chem. Rev.* **2021**, 121 (9), 5417–5478.